Spin noise spectroscopy to probe quantum states of ultracold fermionic atom gases

Bogdan Mihaila,[1] Scott A. Crooker,[2] Krastan B. Blagoev,[1] Dwight G. Rickel,[2] Peter B. Littlewood,[3] and Darryl L. Smith[1]
[1]*Theoretical Division, Los Alamos National Laboratory, Los Alamos, New Mexico 87545, USA*
[2]*National High Magnetic Field Laboratory, Los Alamos National Laboratory, Los Alamos, New Mexico 87545, USA*
[3]*Cavendish Laboratory, Madingley Road, Cambridge CB3 0HE, United Kingdom*
(Received 2 March 2006; published 7 December 2006)

We theoretically demonstrate that optical measurements of electron spin noise can be a spectroscopic probe of the entangled quantum states of ultracold fermionic atom gases and unambiguously reveal the detailed nature of the underlying interatomic correlations. Different models of the effective interatomic interactions predict entirely new sets of resonances in the spin noise spectrum. Once the correct effective interatomic interaction model is identified, the detailed noise line shapes of the spin noise can be used to constrain this model. We estimate the magnitude of spin noise signals expected in ultracold fermionic atom gases via noise measurements in classical alkali vapors, which demonstrate the feasibility of this approach.

DOI: 10.1103/PhysRevA.74.063608 PACS number(s): 03.75.Hh, 03.75.Ss, 05.30.Fk

Ultracold alkali atoms [1] provide experimentally accessible model systems for probing quantum states that manifest themselves at the macroscopic scale. Recent experimental realizations of superfluidity in dilute gases of ultracold fermionic (half-integer spin) atoms [2] offer exciting opportunities to directly test theoretical models of related many-body fermion systems that are inaccessible to experimental manipulation, such as neutron stars [3] and quark-gluon plasmas [4]. Ultracold atoms also offer the possibility to create complex multilevel superfluids by moving into regimes beyond those describable by effective single-channel models [5–7], especially when one is exactly tuned to a Feshbach resonance. Although the thermodynamic evidence for such states is not yet evident in currently studied systems, in fact as we shall see, the signatures are principally spectroscopic. Moreover, however weak such phenomena may be, they introduce qualitatively new fluctuations and represent distinct forms of entanglement.

In this paper, we theoretically demonstrate that optical measurements of electron-spin noise [8,9]—the intrinsic, random fluctuations of electron spin—can be a spectroscopic probe of the entangled quantum states of ultracold fermionic atom gases. The spin noise spectra unambiguously reveal the detailed nature of the interatomic correlations, thereby identifying the correct underlying model of the interatomic interactions. By direct comparison with spin noise measurements in classical alkali gases, we estimate the magnitude of spin noise signals expected in ultracold fermionic atom gases, and demonstrate the feasibility of this approach.

The excitation spectra of physical systems are often studied by measuring their response to an external perturbation. Alternatively, measuring the spectrum of intrinsic fluctuations of a physical system can provide the same information, and these "noise spectroscopies" often disturb the physical system less strongly and scale more favorably with system size reduction. At very low temperatures, noise from quantum fluctuations of an observable that does not commute with the Hamiltonian of the system can be used as a probe of the system properties. Because of the hyperfine coupling, the electron spin is not a good quantum number in alkali gases, and fluctuations of electron spin can be measured using optical Faraday rotation. The electron spin noise spectrum consists of a series of resonances occurring at frequencies corresponding to the difference between hyperfine/Zeeman atomic levels. The integrated strength of the lines gives information about the occupation of the atomic levels, while the line shapes depend on the properties of the condensed atomic state. It is precisely the spectroscopic nature of the electron spin noise measurement that allows one to distinguish between various many-body models for the quantum states of ultracold fermionic atom gases: different models predict entirely different sets of resonances in the noise spectrum, and once the correct effective interatomic interaction model is identified, the line shapes of the spin noise can be used to constrain this model.

To measure the electron spin noise via Faraday rotation spectroscopy, a linearly polarized laser beam, with photon energy tuned near but not exactly on the *s*-*p* optical transition of the outer *s*-orbital electron, traverses an ensemble of alkali atoms [8]. The rotation angle of the laser polarization traversing the sample is measured as a function of time. The noise power spectrum of the rotation angle shows distinct peaks. In the electronic ground state (*s* orbital) there is a strong hyperfine coupling between the nuclear and electron spins. For the electronic *p* orbital, the hyperfine splitting is weak, however there is a strong spin-orbit coupling between the *p* orbital and its spin. The laser photons directly couple to the spatial part of the electron wave function, but because of the spin-orbit splitting in the final state of the optical transition there is an indirect coupling between the laser photons and the electron spin. A fluctuating birefringence, that is, a difference in refractive index for left- and right-hand circular polarizations, results from quantum fluctuations in the electron spin and leads to rotation of the polarization angle of the laser. The experiment is sensitive to fluctuations of electron-spin projection in the direction of laser propagation.

The Hamiltonian describing a system of alkali atoms consists of a sum of one- and two-atom terms. The one-atom Hamiltonian includes the kinetic energy, the Zeeman interaction, and the hyperfine interaction between the nuclear spin $\vec{I}$ and the electron spin $\vec{s}$. The single-atom eigenvectors, the starting point for describing the many-body system, are obtained by diagonalizing the one-atom Hamiltonian. This

Hamiltonian preserves the projection of total angular momentum, $\vec{F}=\vec{s}+\vec{I}$, in the direction of the applied magnetic field. The one-atom matrix elements can be grouped into two-dimensional blocks involving the basis states $|Im_I\rangle|\frac{1}{2}\frac{1}{2}\rangle$ and $|Im_I+1\rangle|\frac{1}{2}-\frac{1}{2}\rangle$, except for the states $|I,m_I=+I\rangle|\frac{1}{2}\frac{1}{2}\rangle$, and $|I,m_I=-I\rangle|\frac{1}{2}-\frac{1}{2}\rangle$, which do not couple. The single-atom energies vary smoothly and do not cross with increasing magnetic field so the single-atom states can be labeled unambiguously by $|Fm_F\rangle$, where m_F is a good quantum number, but F is only a good quantum number at zero magnetic field.

For a linearly polarized optical beam with a Gaussian profile, the spectral density of polarization angle noise is [10]

$$\frac{\phi_N(\omega)}{\sqrt{\delta f}} = C\left[\frac{L\rho_0}{A}S(\omega)\right]^{1/2}, \tag{1}$$

where

$$C = \frac{2\pi}{3}\frac{cr_0}{m_0}\frac{1}{\hbar\Omega}\frac{|\langle S|p_x|P_x\rangle|^2}{|\Omega_{s\text{-}p}-\Omega|}. \tag{2}$$

Here ρ_0 is the density of atoms, Ω is the angular frequency of the laser, $\Omega_{s\text{-}p}$ is the angular frequency of the optical resonance, r_0 is the classical electron radius, m_0 is the electron mass, c is the speed of light, $\langle S|p_x|P_x\rangle$ is the momentum matrix element for the optical transition, and the optical beam area is $A=2\pi R_0^2$ where R_0 is the radius at which the beam intensity drops to $1/e$ of its peak value. The electron-spin response function $S(\omega)$ is

$$S(\omega) = \frac{1}{\rho_0}\int dt e^{i\omega t}\int d^3r\langle\sigma_z(\mathbf{r},t)\sigma_z(0,0)\rangle, \tag{3}$$

where z is the direction of laser propagation, $\sigma_z(\mathbf{r},t)$ is twice the z projection of the electron-spin density operator, and $S(\omega)$ satisfies the sum rule $\int d\omega S(\omega)=2\pi$. The spin response function $S(\omega)$ has peaks at frequencies near the separation between single-atom spin levels

$$S(\omega) = \sum_{ij}|\langle i|\sigma_z|j\rangle|^2 S^{i\to j}(\omega), \tag{4}$$

where $\{i,j\}$ label the single-atom spin levels, $|\langle i|\sigma_z|j\rangle|^2$ is a one-atom matrix element that determines line strengths and selection rules, and $S^{i\to j}(\omega)$ contains information about the many-body state. The response function $S^{i\to j}(\omega)$ is zero unless at least one of the states i or j has nonzero occupation. For laser propagation orthogonal to the magnetic field the selection rules require that the one-atom quantum number, m_F change by ± 1 between the two single-atom levels.

Equations (1) and (2) show that the noise signal decreases linearly with inverse frequency detuning from the optical resonance. By contrast, the energy dissipated into the atomic system, either by optical absorption or Raman scattering, decreases quadratically with inverse frequency detuning. Thus noise spectroscopy measurements are weakly perturbative in the sense that the noise spectroscopy signal decreases more slowly with inverse frequency detuning than does the energy dissipated into the system.

Spin noise spectroscopy measurements will provide interesting information about the underlying interatomic interaction in fermionic gases of either ^{6}Li ($I=1$) or ^{40}K ($I=4$) atoms. Here, we specifically consider the ^{40}K system, which is particularly promising for studying multilevel fermionic models [6]: For ^{40}K the subspace of interacting atomic states is very restrictive, because the hyperfine coupling constant is negative so that the lowest energy state is $m_F=-\frac{9}{2}$. Experimentally, ^{40}K atoms are trapped in the two lowest hyperfine states, $|\frac{9}{2},-\frac{9}{2}\rangle$ and $|\frac{9}{2},-\frac{7}{2}\rangle$. In the s-wave limit, the open channel can couple to only *one* closed-channel state $|\frac{7}{2},-\frac{7}{2}\rangle$, and the interacting part of the Hamiltonian reduces to a three-level system. Figure 1 shows the schematic of the ^{40}K Zeeman structure, the one-atom matrix elements [see Eq. (4)] and corresponding resonance frequencies, at the magnetic field of the Feshbach resonance ($B=202$ G). We denote the atomic states $|\frac{9}{2},-\frac{9}{2}\rangle$, $|\frac{9}{2},-\frac{7}{2}\rangle$, and $|\frac{7}{2},-\frac{7}{2}\rangle$, as 1, 2, and 18, respectively.

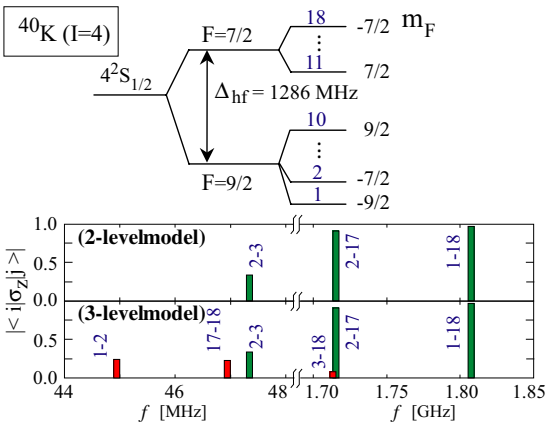

FIG. 1. (Color online) (Top) Zeeman structure of ^{40}K ($I=4$). In the two-level theoretical model of the condensate, only the two lowest hyperfine states are occupied. In the three-level model [6], states 1, 2, and 18 are occupied. (Bottom) The one-atom matrix elements $|\langle i|\sigma_z|j\rangle|$, which determine the spin-response function $S(\omega)$ [see Eq. (4)], and corresponding frequencies, at the magnetic field of the Feshbach resonance ($B=202$ G). In the two-level model, lines 17–18 and 3–18 are forbidden, and line 1–2 has zero strength. Lines 3–18 and 2–17 are almost degenerate.

In the two-level model [11,12], the noise spectrum consists of lines corresponding to occupied-to-occupied and occupied-to-unoccupied states transitions. We use the Hartree-Fock–Bogoliubov (HFB) formalism to calculate the zero-temperature spin-spin response functions $S^{i\to j}(\omega)$. We find that the spin-spin response function corresponding to a transition between two occupied states is

$$S^{1\to 2}(\omega) = \frac{1}{\rho_0}N(k_E)[(1-\rho_{k_E})\rho_{k_E}-\kappa_{k_E}^2]_{E=(\omega-\delta_{12})}, \tag{5}$$

where $N(k)$ is the density of states, and $\rho_k=\langle a_k^\dagger a_k\rangle$ and $\kappa_k=\langle a_k a_k\rangle$ are the normal and anomalous densities, respectively. In Eq. (5) we denote by δ_{12} the energy separation between levels 1 and 2. Since for any k value, $\rho_k^2+\kappa_k^2=\rho_k$, the strength of the $1\to 2$ (occupied-to-occupied) transition vanishes in the two-level model. The vanishing strength of the (occupied-to-occupied) transition is a consequence of the

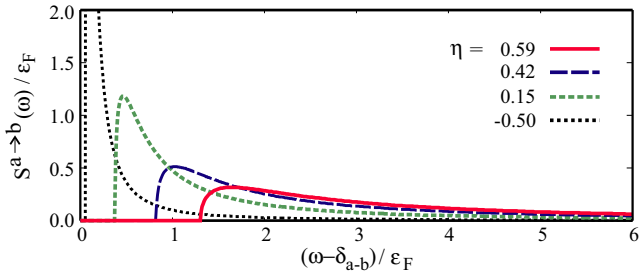

FIG. 2. (Color online) Calculated line shapes for occupied-to-unoccupied transitions in the two-level model, as a function of the dimensionless parameter $\eta=(k_F a)^{-1}$ (where k_F is the Fermi momentum and a is the s-wave scattering length). Occupied-to-occupied transitions have zero strength in the two-level model [13]. In an ultracold gas of potassium atoms with a density (ρ_0) of 10^{13} cm^{-3} the Fermi energy is $\varepsilon_F \approx 5.6$ kHz.

Pauli exclusion principle for a system with two equally populated atomic spin states [13], just as for the noninteracting system. If the two occupied states were not equally populated, the transition strength would not vanish. In the case of a transition from an occupied (a) to an unoccupied state (b), the corresponding spin-spin response function becomes

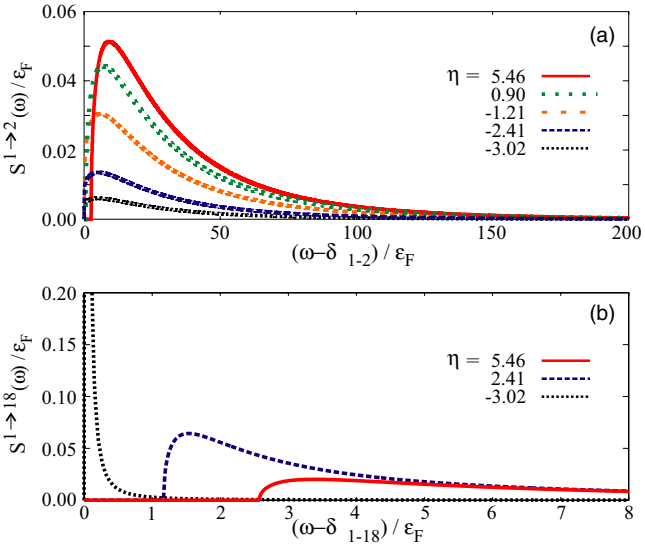

FIG. 3. (Color online) Examples of line shapes in the three-level model discussed in Ref. [6] for ^{40}K: $S^{1\to 2}$ and $S^{1\to 18}$ transitions, respectively. The line shapes depicted in panel (a) have no correspondent in the two-level model, whereas the line shapes depicted in panel (b) correspond to the line shapes shown in Fig. 2. The intensity reduction by an order of magnitude of the lines in the three-level model with respect to the case of the two-level model is a direct consequence of the sum rule obeyed by $S(\omega)$, $\int d\omega S(\omega) = 2\pi$, i.e., the presence of more lines in the noise spectrum leads to a reduced intensity. Finally, the different energy scale of the line shapes in panels (a) and (b) reflect the long-versus short-range nature of the correlations involving the open and closed channels, respectively (see Ref. [6] for further discussions).

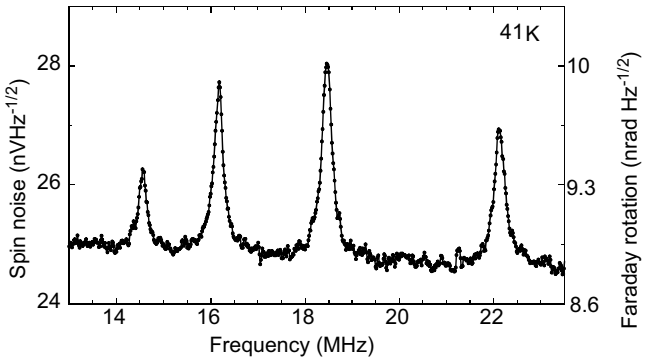

FIG. 4. Spectra of spin noise, measured via Faraday rotation, in a ^{41}K vapor at 184 °C (density $N=7.3\times10^{13}$ cm^{-3}). Peaks correspond to $\Delta m_F=\pm1$ transitions. The probe laser (4 mW) is detuned 100 GHz from the D1 transition ($4S_{1/2}$-$4P_{1/2}$; 770 nm), and $B_\perp = 25.6$ G. The vapor is contained in a 10-mm-long cell, and the laser beam diameter (to $1/e$ peak intensity) is 65 μm. The noise data are shown in units of voltage (nV Hz$^{-1/2}$), and Faraday rotation fluctuations (nrad Hz$^{-1/2}$). The white-noise floor is primarily from photon shot noise and amplifier noise. The discrete peaks show noise from electron-spin fluctuations and have integrated values of 1.3, 2.3, 2.6, and 2.1 μrad. Similar signal magnitudes are expected in ultracold atom systems (see the text).

$$S^{a\to b}(\omega) = \frac{1}{\rho_0}[N(k_E)\rho_{k_E}]_{E_k+(\epsilon_k-\mu)=\omega-\delta_{ab}}, \tag{6}$$

where μ is the chemical potential such that $N_1=N_2=\rho_0/2$. In Fig. 2 we depict the line shape of the occupied-to-unoccupied transitions calculated in the two-level model as a function of the dimensionless parameter $\eta=(k_F a)^{-1}$. Here k_F is the Fermi momentum and a is the s-wave scattering length. In the normal phase ($a\to-0$), the line shape of an occupied-to-unoccupied transition becomes a delta function located at the energy separation between levels 1 and 2. On the BCS side, the quasiparticle dispersion exhibits a local minimum at a finite momentum value, and the corresponding singularity in the density of states [12] is reflected by the characteristic shape of the spin-spin correlation function [14]. On the BEC side of the crossover the singularity in the density of states is located at zero momentum, and the spin-spin correlation function has a smooth shape.

The three-level model discussed in Ref. [6] involves the lowest two hyperfine levels, 1 and 2, plus the topmost hyperfine state denoted by 18. In this model, the particle number constraint becomes $N_1=N_2+N_{18}=\rho_0/2$. Figure 3 shows the characteristic shape of the lines predicted by the three-level model as a function of the dimensionless parameter $\eta=(k_F a)^{-1}$. The top panel illustrates the line shapes of the $1\to2$ transition, whereas the line shapes of the $1\to18$ transition are shown in the bottom panel. The contrast between the predictions of the two-level and the three-level models is evident: In the two-level model, the transitions between the occupied levels, $1\to2$, have zero strength independent of η, while in the three-level model the strength of the $1\to2$ transitions is *nonzero*. This is a consequence of the unequal population of levels 1 and 2 in the three-level model. Tran-

sitions $17 \rightarrow 18$ and $3 \rightarrow 18$ are allowed in the three-level model, but not in the two-level model.

In the last section we show that the expected signal magnitudes are measurable. Because of the sum rule $\int S(\omega) d\omega = 2\pi$, the expected spin noise signals in ultracold atom gases can be directly estimated from corresponding measurements in classical alkali gases. The theoretical results and scaling prefactors of Eq. (1) apply equally to both classical *and* quantum gases. Further, the optical matrix elements and other terms in the prefactors (2) are the same for the isotopes of a given alkali atom. Therefore, we measure spin noise spectra in a classical vapor of ^{41}K atoms (see Fig. 4). The four discrete peaks, with amplitudes of order 1 nrad/Hz$^{1/2}$ above the white-noise floor, result from electron-spin fluctuations between adjacent Zeeman-split hyperfine levels ($\Delta m_F = \pm 1$). The integrated spin noise of the four peaks are 1.3, 2.3, 2.6, and 2.1 μrad, respectively. The ratios of the measured integrated spin noise powers compare well with the theoretical results from Eq. (1). The overall magnitude of the detected spin noise is about a factor 2 lower than theoretical expectation, which may result from uncertainties in the laser beam diameter. In an ultracold gas of potassium atoms with a density of 10^{13} cm^{-3} and a trap length of 0.2 mm, we expect a similar magnitude for the noise peaks with a 20-μm-diam laser detuned 15 GHz from the optical resonance. In ultracold atom gases the laser detuning can be significantly less than 15 GHz and thus much larger noise signals than shown in Fig. 4 should be achievable.

In summary, we have shown that electron-spin noise spectroscopy can be a spectroscopic probe of the quantum states of ultracold atom gases. These measurements have the unique ability to unambiguously reveal the spin entanglement of various many-body quantum states of these systems. In the specific case of ^{40}K, we demonstrate that weak fluctuations beyond the single-channel description are measurable spectroscopically, even though the single-channel description is believed to be very accurate for thermodynamic properties. We specifically considered fermionic atomic gases, but since the existence of multiple transitions is a signature of entanglement of the spin degrees of freedom, the basic approach should apply equally well to other more complex systems.

We thank M. M. Parish and A. V. Balatsky for valuable discussions and acknowledge support from the LDRD program at Los Alamos National Laboratory. B.M. acknowledges support from the ICAM program.

[1] M. H. Anderson *et al.*, Science **269**, 198 (1995); K. B. Davis *et al.*, Phys. Rev. Lett. **75**, 3969 (1995); C. C. Bradley, C. A. Sackett, J. J. Tollett, and R. G. Hulet, *ibid.* **75**, 1687 (1995); B. DeMarco and D. S. Jin, Science **285**, 1703 (1999).

[2] C. A. Regal, M. Greiner, and D. S. Jin, Phys. Rev. Lett. **92**, 040403 (2004); M. Bartenstein *et al.*, *ibid.* **92**, 203201 (2004); M. W. Zwierlein *et al.*, *ibid.* **92**, 120403 (2004); M. W. Zwierlein *et al.*, Nature (London) **435**, 1047 (2005); C. Chin *et al.*, *ibid.* **305**, 1128 (2004).

[3] D. G. Yakovlev and C. J. Pethick, Annu. Rev. Astron. Astrophys. **42**, 169 (2004).

[4] H. Meyer-Ortmanns, Rev. Mod. Phys. **68**, 473 (1996).

[5] M. Holland, S. J. J. M. F. Kokkelmans, M. L. Chiofalo, and R. Walser, Phys. Rev. Lett. **87**, 120406 (2001); E. Timmermans, K. Furuya, P. W. Milonni, and A. K. Kerman, Phys. Lett. A **285**, 228 (2001).

[6] M. M. Parish, B. Mihaila, B. D. Simons, and P. B. Littlewood, Phys. Rev. Lett. **94**, 240402 (2005).

[7] G. M. Bruun, A. D. Jackson, and E. E. Kolomeitsev, Phys. Rev. A **71**, 052713 (2005).

[8] S. A. Crooker, D. G. Rickel, A. V. Balatsky, and D. L. Smith, Nature **431**, 49 (2004).

[9] M. Oestreich, M. Römer, R. J. Haug, and D. Hägele, Phys. Rev. Lett. **95**, 216603 (2005).

[10] B. Mihaila, S. A. Crooker, D. G. Rickel, K. B. Blagoev, P. B. Littlewood, and D. L. Smith, Phys. Rev. A **74**, 043819 (2006); e-print cond-mat/0604522.

[11] A. J. Leggett, in *Modern Trends in the Theory of Condensed Matter*, edited by A. Pekalski and R. Przystawa (Springer-Verlag, Berlin, 1980); C. Comte and P. Nozières, J. Phys. (Paris) **43**, 1069 (1982); P. Nozières and S. Schmitt-Rink, J. Low Temp. Phys. **59**, 195 (1985).

[12] M. M. Parish, B. Mihaila, E. M. Timmermans, K. B. Blagoev, and P. B. Littlewood, Phys. Rev. B **71**, 064513 (2005).

[13] B. Mihaila, S. Gaudio, K. B. Blagoev, A. V. Balatsky, P. B. Littlewood, and D. L. Smith, Phys. Rev. Lett. **95**, 090402 (2005).

[14] Similar line shapes were noted by H. P. Büchler, P. Zoller, and W. Zwerger, Phys. Rev. Lett. **93**, 080401 (2004); R. B. Diener and T.-H. Ho, e-print cond-mat/0405174.